Direct Phase Correction of Differential FT-IR Spectra

M. SHANE HUTSON and MARK S. BRAIMAN*

Department of Biochemistry and Biophysics Program, University of Virginia Health Sciences Center #440, Charlottesville, Virginia 22908

Step-scan transient Fourier transform infrared (FT-IR) difference spectra are often measured in an ac-coupled configuration. The resulting differential intensity spectra contain both positive and negative bands. This condition poses problems for direct phase correction by the standard Mertz and Forman methods. Restricting the calculated phase angle to the range $[-\pi/2, \pi/2]$ was previously shown to fix some of these problems, but we show that the use of a reduced-resolution phase spectrum can produce other artifacts. The effect of reduced resolution is analyzed for a simulated noise-free spectrum and for a measured transient spectrum of a real photochemical system, bacteriorhodopsin. Examination of these results reveals that the Mertz and Mertz Signed methods can produce spectral bands of reduced magnitude and unusual band shape, with considerable amounts of intensity remaining along the imaginary axis after phase correction. However, these errors can be eliminated by self-convolution of the measured interferogram, which doubles all phase angles, prior to smoothing. This procedure removes the potential discontinuities in the phase angle due to sign changes in the differential spectrum. With bacteriorhodopsin, this doubled-angle method for direct phase correction is able to produce a transient spectrum which closely matches that produced by using a separately measured dc interferogram to calculate the phase angle.

Index Headings: **Step-scan difference spectroscopy; Doubled angle; Interferogram self-convolution; Phase resolution.**

INTRODUCTION

In step-scan transient Fourier transform infrared (FT-IR) difference spectra of biological samples, the time-dependent intensity changes are 2–3 orders of magnitude smaller than the static intensity. To measure these intensity changes with maximum sensitivity, it is advantageous to ac-couple the detector.[1] The resulting spectra contain both positive and negative intensities, which are not handled correctly by the standard Mertz and Forman phase correction algorithms.[2,3]

When the spectrum contains regions of positive and negative intensity, these phase correction methods fail to produce the true spectrum. A negative intensity can be interpreted in either of two ways due to the equality:

$$(-A)e^{i\theta} = Ae^{i(\theta+\pi)}. \quad (1)$$

The Mertz and Forman algorithms implicitly assume that most of the intensity in the spectrum is positive. When negative intensities are present, they are likely to be misinterpreted as positive intensities with a phase shift of π radians. However, the phase-angle errors are not limited to π shifts. As demonstrated below, the use of resolution-reducing smoothing procedures leads to a more complicated set of errors.

A popular solution to this problem has been to measure a separate dc-coupled interferogram from which the phase information can be extracted.[4,5] A disadvantage of this approach is that care must be taken to ensure instrument stability between these two measurements. Alternatively, one can measure the two interferograms concurrently with special hardware.[6,7]

To circumvent the need for a separate dc-coupled interferogram, McCoy and de Haseth proposed a modification of the Mertz algorithm for vibrational circular dichroism spectra,[8] which also have positive and negative peaks. This phase correction method has been incorporated into some commercial software applications as the ''Mertz Signed'' method.[9] The broad difference bands of quarterwave plate/polarizer spectra were shown to be properly phase corrected with this algorithm.[8] However, as shown below, this method does not work nearly as well on spectra that have narrow bands of alternating positive and negative intensity. This situation is often encountered in time-resolved step-scan spectroscopy as well as other step-scan methods and vibrational circular dichroism.[4–7]

In light of these shortcomings, we propose here a different method for phase correcting spectra with alternating positive and negative bands, based on doubling the phase angles prior to lowering the resolution. The advantage of doubling the phase angles is that the phase factor $e^{i2\theta}$ is identical for θ and $\theta + \pi$. This benefit eliminates all the potential π flips in the phase. Comparison of this method with the Mertz and Mertz Signed methods shows that our new approach eliminates the phase artifacts associated with the latter two methods. The doubled-angle phase correction method is capable of producing time-resolved step-scan spectra that match those produced with the dc Stored Phase method, without the need for a separate experimental measurement. This new phase correction method may also find utility in phase correction of other types of FT-IR spectra that display both positive and negative bands.

THEORY

Optical and electronic factors can introduce odd (sine) components into the ideally even (cosine) interferogram.[1] Thus, Fourier transformation of the interferogram produces a complex result. Phase correction algorithms are designed to rotate each complex value in this representation of the spectrum onto the real axis. With the Mertz correction method, the frequency-dependent phase angle, $\theta'(\tilde{\nu})$, is calculated from a short double-sided region of the interferogram around the position of zero path difference (ZPD). The phase correction can be represented as

$$B(\tilde{\nu}) = [b(\tilde{\nu})e^{i\theta(\tilde{\nu})}]\, e^{-i\theta'(\tilde{\nu})} \quad (2)$$

where $b(\tilde{\nu})e^{i\theta(\tilde{\nu})}$ is the complex spectrum obtained by Fourier transformation of the interferogram. As long as $\theta(\tilde{\nu})$

Received 29 December 1997; accepted 30 March 1998.

* Author to whom correspondence should be sent.

0003-7028/98/5207-0974$2.00/0

is slowly varying, then $\theta'(\tilde{\nu}) \cong \theta(\tilde{\nu})$, and the Mertz phase correction method produces the true spectrum, with only noise remaining in the imaginary part of the spectrum.

The assumption that $b(\tilde{\nu}) > 0$ with the Mertz algorithm means that negative intensities can result in erroneously calculated phase angles of $\theta'(\tilde{\nu}) = \theta(\tilde{\nu}) + \pi$. Substituting into the above equation,

$$B(\tilde{\nu}) = b(\tilde{\nu})e^{i\theta(\tilde{\nu})}e^{-i(\theta(\tilde{\nu})+\pi)} = b(\tilde{\nu})e^{-i\pi} = -b(\tilde{\nu}). \quad (3)$$

Thus, peaks in some ranges of the phase-corrected spectrum may be incorrectly signed because of the π radians phase error.

Mertz Signed Algorithm. A modification of the Mertz phase correction algorithm designed to handle the positive and negative peaks of vibrational circular dichroism spectra was proposed by McCoy and de Haseth.[8] This method limits the possible phase angles to the range $-\pi/2$ to $\pi/2$. Thus, the π flips in the phase angle caused by negative intensities are reversed by disallowing phase angles in the second and third quadrants. Of course, with a poor choice of the ZPD position, proper phase correction would require phase angles outside the allowed range. However, with the limited phase angle dispérsion produced by carefully engineered interferometers in modern FT-IR spectrometers, there exists a proper choice for the ZPD that allows the Mertz Signed algorithm to map the phase angles of all negative-intensity bands to $\theta'(\tilde{\nu}) = (\theta(\tilde{\nu}) + \pi) - \pi$, so that the phase correction produces the true spectrum.

Nevertheless, as discussed below, lowering the resolution of the phase spectrum to improve the signal-to-noise ratio can result in phase errors of intermediate values; i.e., $\theta(\tilde{\nu}) < \theta'(\tilde{\nu}) < \theta(\tilde{\nu}) + \pi$. In these cases, the Mertz Signed method does not produce the true spectrum.

Phase Correction of a Simulated Interferogram. To demonstrate the errors caused by lowering the resolution to calculate the phase spectrum, we construct a simulated difference interferogram $I(x)$, corresponding to eight differential intensity band pairs of varying spacing, as follows:

$$I(x) = \sum_{j=1}^{8}\left[\cos[2\pi x\tilde{\nu}_j + \theta(\tilde{\nu}_j)] - \frac{1}{2}\cos[2\pi x\cdot(\tilde{\nu}_j + \Delta\tilde{\nu}_j) + \theta(\tilde{\nu}_j + \Delta\tilde{\nu}_j)]\right] \quad (4)$$

where

$$\tilde{\nu}_j = j\cdot(200\ \text{cm}^{-1}), \quad (5)$$

$$\Delta\tilde{\nu}_j = 46\ \text{cm}^{-1} + j\cdot(2\ \text{cm}^{-1}) \quad (6)$$

and

$$\theta(\tilde{\nu}) = \pi/2\cdot(\tilde{\nu} - 1000\ \text{cm}^{-1})^2. \quad (7)$$

With the use of Happ–Genzel apodization and a phase correction angle $\theta'(\tilde{\nu})$ taken directly from the above definition of $\theta(\tilde{\nu})$, the spectrum calculated from the simulated interferogram is shown in Fig. 1A. The double-sided interferogram used for this calculation contains 1000 points with a discrete spacing of 2.5 μm, for a spectral resolution of 8 cm^{-1} over a bandwidth of 0–2000 cm^{-1}.

Calculation of the same spectrum by using the Mertz phase correction method at a phase resolution of 128 cm^{-1} (instead of relying on our *a priori* knowledge of the phase angle) results in the characteristic ''reflected peaks'' pattern for some of the negative bands (Fig. 1B). However, the negative components at 248, 450, and 652 cm^{-1} remain unreflected. It is only the more widely spaced differential band pairs at higher frequency that exhibit reflection, with the weaker negative component becoming more completely reflected as the spacing increases.

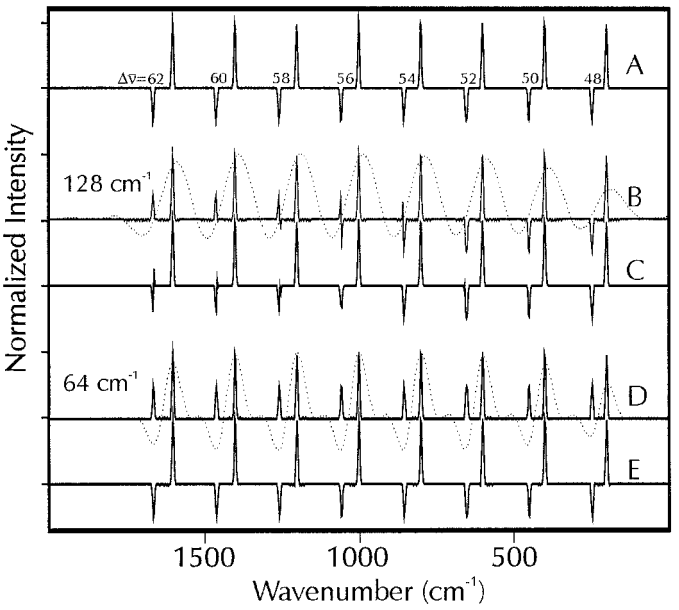

FIG. 1. Phase correction of a simulated difference interferogram, $I(x)$ [see text for the definition of $I(x)$]. (**A**) True spectrum, i.e., spectrum obtained after Fourier transformation and phase correction using the predefined phase angle: $\theta(\tilde{\nu}) = \pi/2(\tilde{\nu} - 1000\ \text{cm}^{-1})^2$. The spacing between each pair of oppositely signed δ functions is listed. (**B**) Spectrum produced by using Mertz phase correction with a phase resolution of 128 cm^{-1}. The *superimposed dotted line* represents the real part of the Fourier transform at 128 cm^{-1} resolution. (**C**) Spectrum produced by using Mertz Signed phase correction with a phase resolution of 128 cm^{-1}. At this resolution the Mertz Signed method is not able to produce the negative bands without error. (**D**–**E**) Spectra corresponding to **B** and **C,** but with 64 cm^{-1} phase resolution. With an increase in the phase resolution, the Mertz Signed method is now able to phase correct the negative bands without error.

Using the Mertz Signed method at 128 cm^{-1} phase resolution (Fig. 1C) orients the peaks in the correct manner qualitatively, but the negative peaks above 1000 cm^{-1} are reduced in magnitude or show unusual band shape. In some cases, the peaks even become split. These artifacts occur when the real part of the Fourier transform at 128 cm^{-1} resolution (dotted line superimposed on Fig. 1B) crosses zero at a frequency within a negative band of the phase-corrected spectrum. When the phase resolution is changed to 64 cm^{-1}, all the negative peaks are reflected in the Mertz phase-corrected spectrum (Fig. 1D). The real part of the Fourier transform at 64 cm^{-1} (dotted line superimposed on Fig. 1D) is <0 in the vicinity of all the negative peaks; thus, the Mertz Signed method is able to properly phase correct the spectrum at this phase resolution (Fig. 1E). However, if the spacing of + and − bands is reduced to $\leq$32 cm^{-1}, the phasing errors and resulting spectral artifacts return (not shown).

These artifacts can be better understood by thoroughly

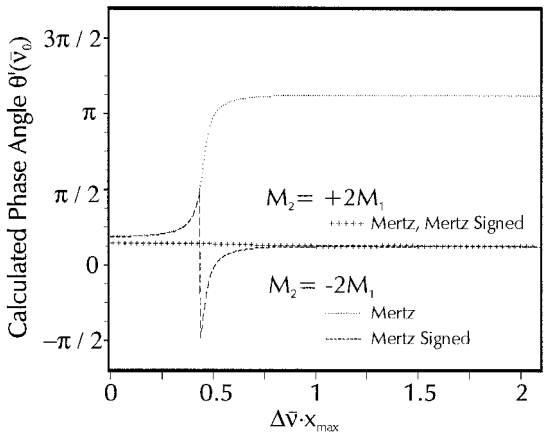

FIG. 2. Effect of a band of intensity $M_2 = \pm 2M_1$ on the phase calculation of a nearby band of intensity M_1. It is assumed that the true phase angles of the bands are $\theta_1 = \pi/8$ and $\theta_2 = 5\pi/32$. The calculated phase angle is plotted as a function of the band separation, $\Delta\bar{\nu}$, normalized by the nominal phase resolution, $1/x_{max}$. If the intensities of both bands are positive ($M_2 = 2M_1$), then with either the Mertz or Mertz Signed algorithm, the calculated phase angle (**plus symbols**) is bounded by $5\pi/32$ and $\pi/8$. However, if the intensities are of opposite sign ($M_2 = -2M_1$), then the phase angle calculated with the Mertz method (**dotted line**) is bounded only by $5\pi/32$ and $9\pi/8$. Application of the Mertz Signed phase correction (ATAN function) restricts the resultant phase angle to the $-\pi/2$ to $\pi/2$ range (**dashed line**), but large errors in the phase angle persist near a discontinuity at $\Delta\bar{\nu}\cdot x_{max} = 0.44$. The band separation near which these errors appear depends on the relative magnitude of the two bands and the apodization function.

examining the phase calculation. The apodized interferogram can be represented as the inverse Fourier transform of the spectrum $b(\bar{\nu})$ times the instrumentally generated phase factor $e^{i\theta(\bar{\nu})}$, all multiplied by the apodization function $A(x)$:

$$I(x) = A(x)\cdot \mathcal{F}^{-1}\{b(\bar{\nu})e^{i\theta(\bar{\nu})}\}. \quad (8)$$

Fourier transformation of this apodized interferogram yields the convolution of the complex spectrum with the line shape function, $L(\bar{\nu}) = \mathcal{F}\{A(x)\}$:

$$B'(\bar{\nu}) = L(\bar{\nu}) \otimes [b(\bar{\nu})e^{i\theta(\bar{\nu})}]. \quad (9)$$

Regardless of the apodization function used, as the resolution of the phase calculation is lowered, $L(\bar{\nu})$ broadens. Therefore, all bands are broadened; i.e., the contribution to the calculated phase angle from neighboring peaks is increased.

Let us now examine in more detail the effects of this contribution using a simplified spectrum consisting of two δ functions of magnitudes M_1 and M_2 at $\bar{\nu}_0$ and $\bar{\nu}_0 - \Delta\bar{\nu}$, respectively. Applying the convolution described above, one obtains

$$B'(\bar{\nu}) = L(\bar{\nu} - \bar{\nu}_0)M_1 e^{i\theta(\bar{\nu}_0)} + L(\bar{\nu} - \bar{\nu}_0 + \Delta\bar{\nu})M_2 e^{i\theta(\bar{\nu}_0 - \Delta\bar{\nu})}. \quad (10)$$

Evaluation of this equation at the center frequency of the band at $\bar{\nu}_0$ gives

$$B'(\bar{\nu}_0) = L(0)M_1 e^{i\theta_1} + L(\Delta\bar{\nu})M_2 e^{i\theta_2} \quad (11)$$

where we have defined $\theta_1 = \theta(\bar{\nu}_0)$ and $\theta_2 = \theta(\bar{\nu}_0 - \Delta\bar{\nu})$. Thus, B' evaluated at the position of one band is actually a weighted vector sum with contributions from both bands.

Figure 2 shows the behavior of the calculated phase angle, θ', as a function of the separation between the two bands, $\Delta\bar{\nu}$, normalized by the phase resolution $1/x_{max}$. If M_1 and M_2 are of the same sign, then the calculated phase angle $\theta'(\bar{\nu}_0)$ at the center of the resolution broadened line is constrained to the range of θ_1 to θ_2 (Fig. 2, solid line). Assuming that the true phase angle varies slowly (i.e., $\theta_1 \approx \theta_2$), the phase errors introduced by using a reduced resolution are small for bands of the same sign.

However, if M_1 and M_2 are of opposite sign, as in the simulated spectrum of Fig. 1, then θ' may vary from θ_2 to $\theta_1 + \pi$ (Fig. 2, dotted line). In the example in Fig. 2, the relative intensity of the neighboring bands is given by $M_2 = \pm 2M_1$. Thus, the intensity in the wings of band 2 exactly cancels the center intensity of band 1 when the band separation is equal to the half-width at half-height (HWHH) of the apodization function. Passing through this separation, the calculated phase angle at ν_0 undergoes a rapid transition of π radians. At much smaller separations, it approaches θ_2; at much larger separations, it approaches $\theta_1 + \pi$.

For the Happ–Genzel function (the apodization function used throughout this paper), $\Delta\bar{\nu}_{HWHH} = 0.44/x_{max}$.[1] When $\Delta\bar{\nu}\cdot x_{max} \ll 0.44$, the calculated phase angle at $\bar{\nu}_0$ is heavily influenced by the larger neighboring band, so that $\theta' \simeq \theta_2$. This is the situation also encountered in Fig. 1B for the bands at 248, 450, and 652 cm^{-1}. In these cases, the neighboring positive band is close enough to the negative band of interest to dominate the phase angle calculation. Thus, no π flip is encountered in the calculated phase angle, and a negative band is properly produced by the Mertz phase correction method.

On the other hand, when $\Delta\bar{\nu}\cdot x_{max} \gg 0.44$, the phase angle calculation is influenced more by the negative band itself, so that $\theta' \simeq \theta_1 + \pi$. This pattern can be seen in Fig. 2, where the dotted line approaches $9\pi/8$ at large separations. All the bands in Fig. 1D also fall into this category. The two oppositely signed bands in each pair are much farther apart than the half-width of the line shape function introduced by resolution reduction and apodization. Thus, the influence of the positive band on the neighboring negative band is small, and a π shift does occur in the calculated phase angle. In this case, the Mertz algorithm produces reflected band shapes.

With the addition of a (second) π shift when $\Delta\bar{\nu}\cdot x_{max} > 0.44$, the Mertz Signed algorithm can often produce a properly phase-corrected spectrum even when the Mertz algorithm fails (Fig. 2, dashed line). This result can also be seen by comparing traces D and E in Fig. 1. However, in the region of $\Delta\bar{\nu}\cdot x_{max} \approx 0.44$, the phase angle θ' calculated with the Mertz Signed algorithm still undergoes large swings away from the true phase angle. The source of these large swings is apparent from Fig. 2. Use of the full-range arctangent function, as in the Mertz method (dotted line), produces a smooth transition from $\theta' \simeq \theta_2$ to $\theta' \simeq \theta_1 + \pi$. Limiting the phase angle to $-\pi/2$ to $\pi/2$ with the ATAN function, as in the Mertz Signed algorithm (dashed line), produces a calculated phase angle in which large errors remain. These large errors occur whenever the phase resolution is chosen in such a way that neighboring bands of unequal intensity and opposite sign nearly cancel one another near the center of the weaker band.

This is precisely the situation encountered for the

peaks above 1000 cm^{-1} in the simulated spectrum of Fig. 1 with a phase resolution of 128 cm^{-1} (traces B and C). The spacing between the peaks at this phase resolution is just large enough to ensure that the positive band can significantly influence, but not dominate, the calculation of the phase angle for the negative band. This pattern can be seen in the 128 cm^{-1} resolution Fourier transform of the interferogram (dotted trace superimposed on Fig. 1B), which shows the nearly complete cancellation of intensity at the centers of these negative bands. The intermediate phase angles that result are manifest as partially reflected peaks in the Mertz-calculated spectrum (Fig. 1B). These errors cannot be properly corrected by application of the Mertz Signed algorithm (Fig. 1C).

While the preceding discussion focuses on phase correction errors with the use of the Mertz method, it is applicable to the Forman method as well. The phase errors resulting from oppositely signed bands occur during the calculation of the phase spectrum, $e^{-i\theta'(\bar{\nu})}$, a step that is common to the Mertz and Forman methods.[2,3]

Phase Correction via Self-Convolution of the Interferogram (Doubled-Angle Method). As shown above, the problems encountered in applying the Mertz Signed algorithm to ac-coupled spectra can be traced to the smoothing of a discontinuous function. However, it is possible to eliminate the discontinuities and thus restore the slowly varying nature of the phase angle, simply by convolving the interferogram with itself prior to carrying out the phase correction. This convolution is equivalent in the Fourier domain to squaring the complex representation of the spectrum, i.e.,

$$\mathcal{F}\{I \otimes I\} = [b(\bar{\nu})e^{i\theta(\bar{\nu})}]^2 = b^2(\bar{\nu})e^{i2\theta(\bar{\nu})}. \quad (12)$$

Thus, the self-convolved interferogram $I \otimes I$ is the inverse Fourier transform of a complex spectrum containing only positive intensities, b^2, and a slowly varying phase angle, $2\theta(\bar{\nu})$. The doubled phase angle, $2\theta'(\bar{\nu})$, can easily be calculated by applying the ATAN2 function to the real and imaginary parts of the Fourier transform of $I \otimes I$. (Note that the algorithm used in the Array Basic program provided in the Appendix does not actually employ the ATAN2 function, but carries out mathematically equivalent operations.) The advantage of performing the self-convolution and thus doubling the phase angles is that the phase factor $e^{i2\theta(\bar{\nu})}$ becomes identical for θ and $\theta + \pi$. This condition eliminates all the π flips in the phase. It is thus possible to truncate and apodize the self-convolved interferogram ($I \otimes I$) prior to Fourier transformation, i.e., to reduce the phase resolution, without introducing any large phase angle errors.

Taking half of the reduced-resolution doubled-phase-angle gives the best smoothed estimate for the phase of the original interferogram. However, determining the half-angle still requires a choice between $\frac{1}{2}[2\theta'(\bar{\nu})]$ and $\frac{1}{2}[2\theta'(\bar{\nu})] + \pi$. This ambiguity can be resolved by using the criterion that the phase angle must be a slowly varying function of $\bar{\nu}$. During the calculation of the discrete array of phase angles, each $\theta'(\bar{\nu})$ is simply chosen to be the value closer to that of the previous element of the array. This choice is now easy because the resolution reduction has suppressed the noise without introducing phase angles between $\theta'(\bar{\nu})$ and $\theta'(\bar{\nu}) + \pi$.

When the entire phase array has been produced, a global choice remains. Adding π to the phase angle at all frequencies also satisfies the criterion of slowly varying phase. The only way to make this choice is by examining the resulting phase-corrected spectrum. Adding π to the phase angle is equivalent to multiplying the entire spectrum by -1. Thus, while the algorithm produces the correct relative orientation of positive and negative peaks, some knowledge of the ''correct'' global orientation of the spectrum is required. With respect to the simulated spectrum of Fig. 1, *a priori* knowledge of the sign of any one band allows proper global orientation of all of them. Thus, without any other information, the Doubled-Angle method can correct the phases of our simulated differential interferogram, producing a result (not shown) that is identical to Fig. 1A.

For the Doubled-Angle phase correction method to work properly, a double-sided interferogram is needed. To see why, consider the effects of truncating one side of a double-sided differential interferogram prior to convolving it with itself. This one-sided truncation introduces erroneous phase angles in the Fourier transform of the unconvolved interferogram; convolution doubles these erroneous angles. Reducing the resolution after convolution smooths the errors slightly but does not significantly reduce them. They can be avoided only by using the full double-sided interferogram to calculate the convolution.

ZPD Selection. The interferogram signal at the ZPD is approximately equal to the spectral intensity integrated over the bandwidth. Thus a spectrum containing positive and negative intensities of comparable magnitude will produce an interferogram without a centerburst at the ZPD. Even in such cases, the ZPD can often be defined from the convolution of the interferogram with itself. The integration of the squared intensities results in a centerburst in the self-convolved interferogram. The position of this centerburst can then be used to locate the ZPD of the original interferogram. If a measured interferogram of N points is represented as $I(n)$ where $n = (0, \ldots, N - 1)$, and $I(n)$ is set to zero for $n < 0$ and $n \geq N$, then the self-convolution is defined as

$$I \otimes I(m) = \sum_{n=0}^{N-1} I(n)I\left(\frac{N}{2} - 1 - n + m\right). \quad (13)$$

(Note: This definition of convolution is dictated by the Array Basic programming language that we used to implement our phase correction method as detailed in the Appendix). According to this definition, if the ZPD is at point $N/2 - 1 + \Delta x$ of the original interferogram, then the self-convolution will shift it to point $N/2 - 1 + 2\Delta x$. If the centerburst of the self-convolved interferogram occurs at a point where $2\Delta x$ is odd, it is rounded down by one so that Δx can be integral.

MATERIALS AND METHODS

Bacteriorhodopsin (bR) samples were prepared from *H. halobium* as described previously.[10] Purple membrane pellets were washed with distilled water and transferred to a CaF_2 window. A second CaF_2 window was coated around its edge with vacuum grease and pressed against the first to seal the bR sample.

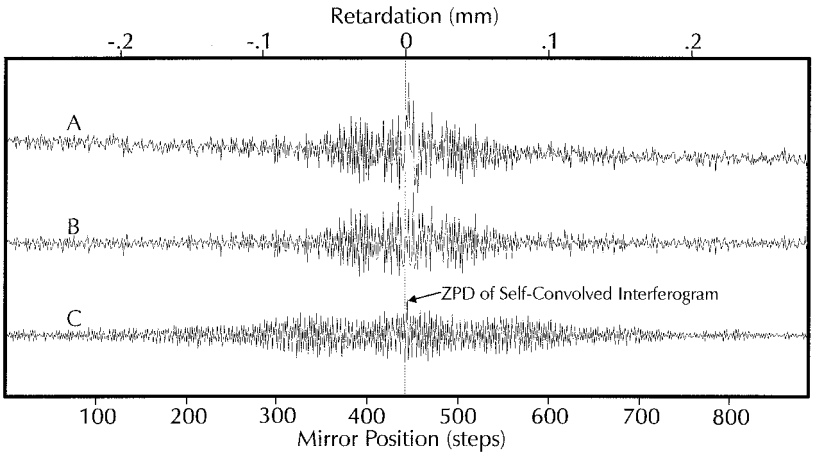

FIG. 3. (**A**) Transient ac-coupled interferogram of bacteriorhodopsin photoproducts averaged over the time range 0–1 ms after photolysis (8 cm^{-1} resolution with a bandwidth of 0 to 1970 cm^{-1}; i.e., a total of 888 points). (**B**) Same interferogram after application of a digital high-pass Fourier filter with a cutoff frequency of 400 cm^{-1}. (**C**) Convolution of the filtered interferogram (**B**) with itself. This self-convolved interferogram has an enhanced intensity at the ZPD (or a nearby point; see text for details) and is therefore used to identify the ZPD of the original interferogram. For the two-sided interferogram in **A**, there are 444 points to the left of the ZPD and 443 to the right. For the self-convolution in **C**, the ZPD is shifted slightly, as calculated by our program, with 445 points to the left and 442 to the right.

Interferograms were collected on a Bruker IFS-66 FT-IR spectrometer in time-resolved step scan mode at 8 cm^{-1} resolution by using a Kolmar photovoltaic HgCdTe detector (Model #KMPV11-1-LJ2/239). This detector's preamplifier has dual ac- and dc-coupled outputs. The measured bandwidth was limited to 0–1970 cm^{-1} as a result of reduced sampling of the interferogram. A long-pass optical filter placed in front of the detector prevented aliasing of optical signals from outside this bandwidth. A pulsed, frequency-doubled Nd^{+}:YAG laser (532 nm, 10 mJ cm^{-2}) was used to trigger the bR photocycle for the transient FT-IR measurements, which were made with the detector and internal digitizer ac-coupled. Transient signals from 10 flashes, spaced every 300 ms, were recorded at each mirror position. Time-resolved interferograms corresponding to 10 time slices of 100 μs each were sorted and stored to disk, but the 10 interferograms were averaged together prior to phase calculation.

To obtain a dc-coupled step-scan interferogram for phase correction with the dc Stored Phase method, we recorded three time slices of 10 ms each with the laser off, with 10 coadditions at each mirror position. The three time slices were then averaged and stored as a single interferogram. This interferogram was measured immediately prior to collection of the ac-coupled differential interferograms to which the stored phase was to be applied.

Data processing of the interferograms was carried out in Array Basic routines on GRAMS/32 software (Galactic Industries, Salem, NH). The Mertz and dc Stored Phase methods for phase correction were implemented by running the standard icompute.ab Array Basic code supplied with the software. The Mertz Signed and Doubled-Angle methods were implemented by simple modifications of icompute.ab, as detailed in the Appendix.

RESULTS

We tested various phase correction methods on typical time-resolved FT-IR data from a biological sample, bacteriorhodopsin. The transient differential interferogram measured from a bR sample after photolysis is shown in Fig. 3A. These data, and the phase correction results obtained from them, are representative of measurements on four different samples of bR.

Determination of the ZPD. There is a sloping baseline in the raw interferogram in Fig. 3A; such a baseline drift is quite common in step-scan measurements. This artifact must be removed by the application of a digital high-pass Fourier filter (Fig. 3B). Failure to remove this sloping baseline results in a self-convolved interferogram with low-frequency features that prohibit selection of the ZPD position (not shown). The self-convolution of the filtered interferogram has a clear centerburst at its ZPD (Fig. 3C). The position of this centerburst is used to define the ZPD of the original interferogram as discussed above.

Comparison of Phase Correction Methods. Figure 4 shows the results of different phase correction algorithms applied to a step-scan time-resolved interferogram of bR photolysis. The same measured differential interferogram (Fig. 3A) and ZPD position were used for all of the phase correction methods. For the Doubled-Angle method, the only *a priori* knowledge of the spectrum that was utilized is the positive sign of the large intensity change at 1527 cm^{-1}.[11] This information is needed to make the correct global choice of sign for the spectrum.

The spectra produced with the dc Stored Phase (A) and Doubled-Angle methods (D) match very closely over the entire 850–1950 cm^{-1} region, while the Mertz algorithm (B) produces a pattern of ''reflected peaks'' over much of the spectrum. The Mertz Signed algorithm (C) corrects some, but not all, of these peaks. The broad area of negative intensity from 1250 to 1450 cm^{-1} is properly phase corrected, but the juxtaposition of positive and negative bands from 1500 to 1600 cm^{-1} causes the Mertz Signed algorithm to produce bands of much reduced intensity, corresponding roughly to a $\pi/2$ phase error.

As a more stringent test of these methods, the residual spectra remaining along the imaginary axis after phase correction were examined (Fig. 5). Both the dc Stored

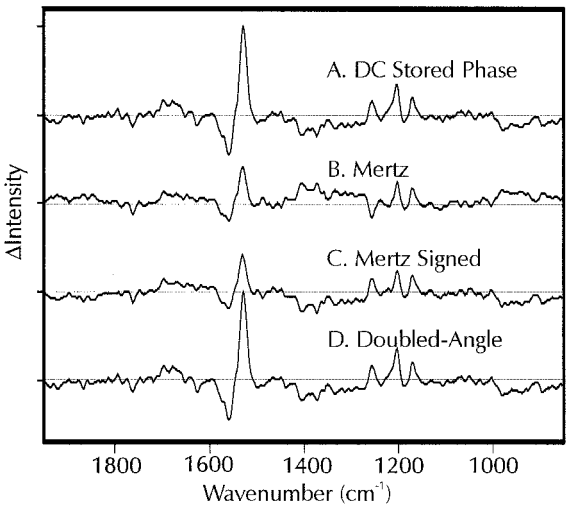

FIG. 4. Phase correction methods applied to calculating the transient ac-coupled spectrum of bR, averaged over the first 1 ms after a photolysis flash. All four traces were computed from the same transient difference interferogram, each using the indicated method of phase correction. The spectral resolution is 8 cm^{-1} over a bandwidth of 0 to 1970 cm^{-1} with Happ–Genzel apodization and 128 cm^{-1} phase resolution. Although the Mertz Signed method corrects some areas of ''reflected peaks'' (1250–1450 cm^{-1}) seen with the Mertz phase correction, it produces bands of reduced magnitude in other regions (1500–1600 cm^{-1}). However, the Doubled-Angle and dc Stored Phase methods produce nearly identical spectra.

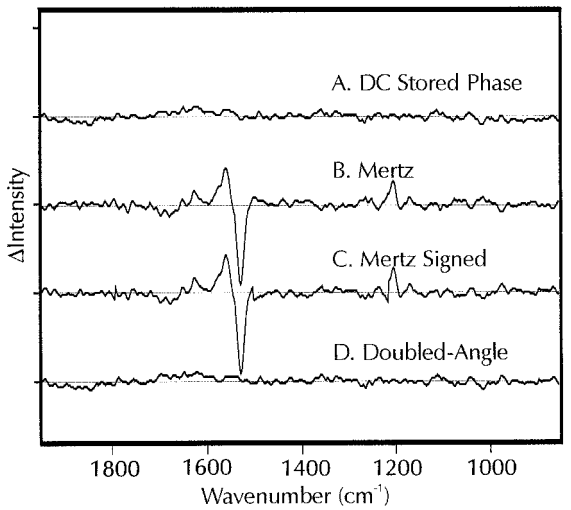

FIG. 5. Residual spectra left along the imaginary axis after phase correction with each of the methods. The scale is the same as in Fig. 4. With either the Mertz or the Mertz Signed method, the residual spectral intensity is as large as the real spectral intensity (Fig. 4) for some bands. On the other hand, the residual intensities of the Doubled-Angle and dc Stored Phase methods are comparable to the noise.

Phase and Doubled-Angle methods produce residual imaginary spectra which appear as random noise. However, the residuals from the Mertz and Mertz Signed methods have features much larger than the noise at 1201, 1527, and 1560 cm^{-1}; these correspond to improperly phase-corrected bands in the real spectra. Note that in the broad region of negative intensity between 1250 and 1450 cm^{-1}, all four methods give residual (imaginary) spectra smaller than the noise. Although the Mertz algorithm succeeds in rotating the differential intensity in this region fully onto the real axis, it incorrectly assigns the sign of that intensity.

The phase spectra produced with the four methods are shown in Fig. 6. The phase angles from both the dc Stored Phase and Doubled-Angle methods are close to zero and vary slowly across the spectrum. However, the phase angles calculated by using the Mertz and Mertz Signed algorithms cover the entire allowed ranges ($[-\pi, \pi]$ and $[-\pi/2, \pi/2]$, respectively). As discussed in the Theory section, with a true phase angle close to 0, the Mertz algorithm applied to a spectrum of alternating positive and negative bands should ideally produce a discontinuous phase spectrum which jumps between 0 and $\pm\pi$ radians. There are hints of such discontinuities in the Mertz phase spectrum (Fig. 6, dot-dash line), but these features are smoothed by the low (128 cm^{-1}) resolution of the phase calculation. Likewise, in the region from 1500 to 1600 cm^{-1}, in which the Mertz Signed algorithm works least effectively, the phase angle takes an intermediate value of $-\pi/2$ instead of 0 or $\pm\pi$ radians.

Effect of Varying the Phase Resolution. As discussed in the Theory section above, the spectral artifacts produced with the Mertz Signed algorithm are due to smoothing of the phase spectrum. The phase angle is calculated from a truncated region of the interferogram and then interpolated to match the point spacing of the spectrum from the full interferogram.

Figure 7A shows how truncating the interferogram at different resolutions affects the real part of its Fourier transform (i.e., the spectrum used for calculating the phase angles). To give accurate phases with the Mertz Signed method, this real part of the Fourier transform generally needs to faithfully reproduce the positions of the zero-crossings of the true intensity spectrum. However, as the phase resolution is lowered from 8 to 32 cm^{-1}

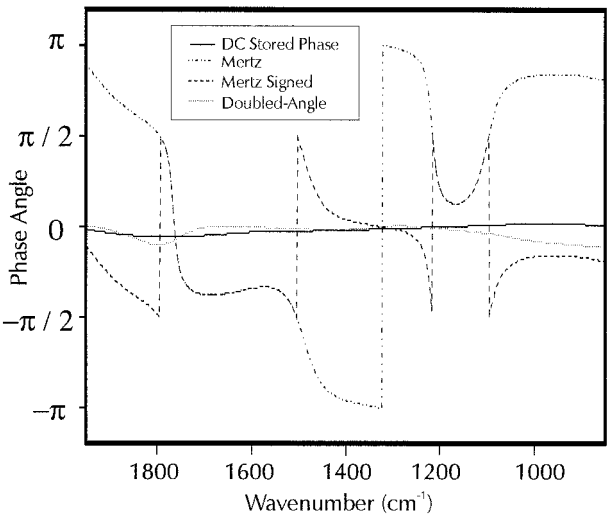

FIG. 6. Phase spectra calculated by using each of the four methods at 128 cm^{-1} phase resolution. Interpolation to the full 8 cm^{-1} spectral resolution was performed by zero-filling the truncated interferogram prior to Fourier transformation. The Mertz method does not simply jump from an angle near 0 for positive bands to an angle near $\pm\pi$ for negative bands. Instead, large regions of the spectrum have calculated phase angles of intermediate values. Restriction of the phase angle to $[-\pi/2, \pi/2]$ with the Mertz Signed method does not restore all phase angles to near 0 because of these intermediate angles. However, the Doubled-Angle method does produce phase angles that vary slowly with $\bar{\nu}$ and are close to 0 everywhere.

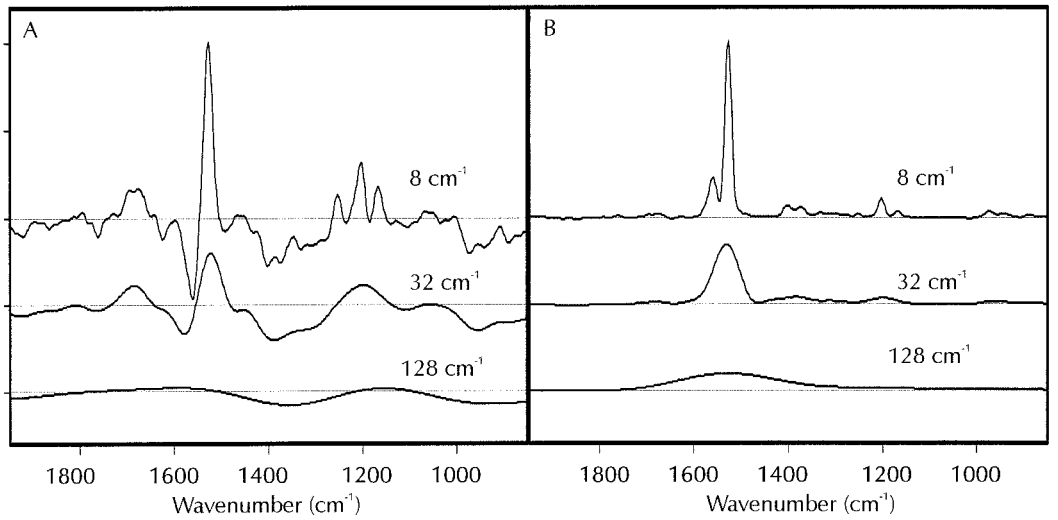

FIG. 7. Behavior, as the resolution is decreased, of the real part of the Fourier transform of (**A**) the original interferogram and (**B**) the self-convolution of the interferogram. No phase correction has been applied.

and then to 128 cm^{-1}, the number of zero-crossings between 850 and 1950 cm^{-1} drops from 17 to 10 to 4, and their positions are shifted. The large positive real band at 1527 cm^{-1} in the high-resolution Fourier transform (Fig. 7A, top trace) corresponds to an area of near zero intensity at 128 cm^{-1} resolution (Fig. 7A, bottom trace). The same is true for the three positive bands near 1200 cm^{-1}. The only consistent feature with a sign that does not depend strongly on spectral resolution is the broad area of negative intensity between 1250 and 1450 cm^{-1}.

In contrast, Fig. 7B shows the real part of the spectrum calculated from the Fourier transform of the self-convolved interferogram. Nearly all intensities are now greater than zero regardless of the resolution used. Although the bands are broadened at 128 cm^{-1} resolution, the positions of the peaks are consistent with the bands observed at 8 cm^{-1} resolution.

For the Mertz Signed method, smoothing due to the reduced resolution of the phase spectrum results in intermediate values of the calculated phase angle $\theta'(\tilde{\nu})$ in regions of sharp alternating positive and negative features in the spectrum (see Fig. 8). The zero-crossings of the real part of the Fourier transform (Fig. 7A) occur at the same wavenumber values as the big jumps in the phase angle (Fig. 8). At 8 cm^{-1} resolution, after application of the $-\pi/2$ to $\pi/2$ limitation, the phase angle $\theta'(\tilde{\nu})$ is close to zero at most frequencies except for those directly adjacent to zero-crossings. Unfortunately, these are made more frequent by spectral noise. At 32 and 128 cm^{-1} resolution, the noise is progressively suppressed, but the phase spectrum is also progressively subject to the systematic errors induced by the broadened line shape (see Theory section).

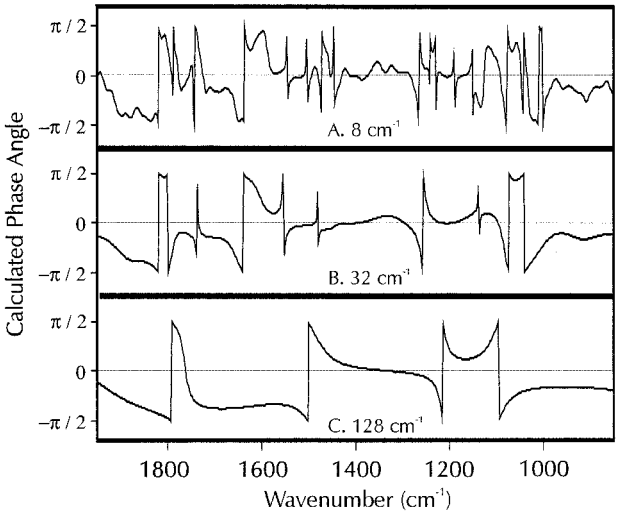

FIG. 8. Phase spectra calculated with the Mertz Signed method at various spectral resolutions. The interferogram was truncated at the indicated resolution, and zero-filled prior to Fourier transformation and phase angle calculation using the formula, $\theta'(\tilde{\nu}) = \mathrm{ATAN}(\mathrm{Im}(\tilde{\nu})/\mathrm{Re}(\tilde{\nu}))$.

The results of these systematic errors can be seen clearly in Fig. 8C. The worst case occurs between 1500 and 1750 cm^{-1}. Here, the phase angle might be expected to flip between ~ 0 and $\sim(\pm\pi)$ for the Mertz method, and to be corrected to ~ 0 everywhere by the Mertz Signed method. Instead the phase angle takes on an intermediate value near $-\pi/2$ over a large spectral range. This value is unaffected by whether the Mertz or Mertz Signed method is used. The resulting spectra (Fig. 4B, 4C) thus coincide in this wavenumber range, but show incorrect magnitudes of both positive and negative bands.

The Mertz and Mertz Signed methods do not diverge over the 1500–1750 cm^{-1} spectral region until the phase resolution is raised to 32 cm^{-1} (spectra not shown). Even at this resolution, however, the negative band at 1560 cm^{-1} still shows a systematic artifact due to the broadening of the large positive neighboring band at 1527 cm^{-1}, analogous to the artifacts shown in Fig. 1C. Only at 8 cm^{-1} resolution does the Mertz Signed method properly correct the phase in the 1500–1750 cm^{-1} range. However, the poorer signal-to-noise ratio in other regions of the spectrum precludes use of this phase resolution for correcting the entire spectral range.

DISCUSSION

The presence of both positive and negative peaks in an FT-IR difference spectrum poses a binary choice of θ or

$\theta + \pi$ for each phase angle for any direct method of phase-correcting a measured differential interferogram. For most FT-IR spectrometer designs, there are two characteristics of the phase spectrum that can be used to make this choice: (1) the phase angle should be everywhere close to zero simultaneously for an appropriately chosen ZPD; and (2) the phase angle should vary slowly as a function of $\tilde{\nu}$.

The three direct methods of phase correction evaluated here—Mertz, Mertz Signed, and Doubled-Angle—each use different criteria for determining the phase angle. The Mertz algorithm assumes that the phase angle varies slowly and that the intensity is always positive except for noise. The latter assumption is clearly incorrect for ac-coupled difference spectra. Use of the Mertz algorithm results in an error of π radians for broad negative bands, and an error near $\pi/2$ radians for regions containing closely spaced positive and negative bands of similar intensity.

The Mertz Signed method substitutes the assumption of positivity with a more realistic criterion for differential spectra, which assumes that the phase angles should all lie within the interval $[-\pi/2, \pi/2]$. Phase factors are thus restricted to lie in the first and fourth quadrants of the complex plane; π radians are added to any calculated angle that falls outside these limits. The method is successful at correcting the reflection of broad negative-intensity peaks. However, it fails to correct spectral regions containing sharp alternating positive and negative bands, frequently yielding a result identical to the Mertz algorithm, i.e., strongly attenuated bands due to an erroneous phase that cannot be corrected by the addition of any multiple of π radians. As we show above, this erroneous phase results from blurring of neighboring positive and negative bands by the use of a lowered phase resolution.

Like the Mertz and Mertz Signed methods, the Doubled-Angle method presented here utilizes a truncated (reduced-resolution and reduced-noise) interferogram to calculate the phase, thereby implicitly assuming a slowly varying phase angle. However, the errors obtained with the Mertz Signed method as a result of blurring sharply alternating positive and negative bands into each other are eliminated by doubling their phase angles prior to blurring. This approach allows nearby bands with phases that differ by nearly π to be smoothed onto each other without introducing erroneous intermediate phase angles, since θ and $\theta + \pi$ give equivalent angles when multiplied by 2. Therefore, the slowly varying nature of the phase spectrum is maintained. There is a binary choice that must be made when the original phase angles are restored by dividing by 2. However, this choice can be made easily because the Doubled-Angle method succeeds in allowing resolution reduction to improve the signal-to-noise ratio in regions of alternating bands, without introducing phase artifacts.

Effect of Noise on Phase Correction. The anomalous phase angles produced with the Mertz and Mertz Signed methods in the presence of positive and negative bands occur at the zero-crossings of the reduced-resolution spectrum. It might therefore be assumed that noise is the culprit. This assumption is true only indirectly. If at certain frequencies the spectral magnitude drops below the noise level, then the phase angle, $\theta'(\tilde{\nu}) = \arctan[\mathrm{Im}(\tilde{\nu})/\mathrm{Re}(\tilde{\nu})]$, becomes indeterminate. However, as shown in the Theory section above, phase errors near zero-crossings can occur even in the complete absence of noise. Therefore, it is not correct to assert that the phase angle errors that occur near the zero-crossings of $\mathrm{Re}(\tilde{\nu})$ with the Mertz Signed method are due to random noise.

It is true that noise-free spectra, such as the simulated spectrum of Fig. 1, can always be properly phase corrected by using the Mertz Signed method, if the phase resolution is increased sufficiently. However, for measured spectra, increasing the phase resolution always increases noise. Thus, at high phase resolution, noise limits the accuracy of the phase angle calculation; at low phase resolution, on the other hand, line shape smoothing introduces phase errors regardless of the amount of noise present.

The Doubled-Angle method eliminates the phase errors produced with alternating signed bands at reduced phase resolution. However, the effect of noise with the Doubled-Angle method can be more severe than with the Mertz methods, especially at high resolution. Thus, the phase correction with the Doubled-Angle method must generally be performed at low phase resolution, typically 128 cm^{-1}.

Direct (Doubled-Angle) Phase Correction vs. the dc Stored Phase Method. In terms of spectral accuracy, our Doubled-Angle phase correction method is comparable to, but does not outperform, the dc Stored Phase method. However, because it is a direct method, there is no need to collect a separate interferogram for the phase calculation. Possible benefits of the direct approach include decreased susceptibility to instrumental drift and less total time required to collect the data.

However, these benefits may be partially negated by the need to use more computer memory to collect double-sided interferograms. This is the only significant drawback of the direct Doubled-Angle phase correction method. This requirement has a cost in terms of disk space and RAM utilization. In addition, the measurement of transient FT-IR step-scan spectra requires a means to perturb the sample reversibly at each of $\sim 10^3$ positions of the moving mirror. The need for double-sided interferograms increases the number of positions required to collect a single interferogram by almost twofold, so that an even greater premium is place on the reversibility of the changes effected by the sample perturbation. However, the signal-to-noise ratio in the final result is improved by collecting a two-sided interferogram. Most step-scan time-resolved experiments require significant signal averaging in any case. Therefore, collecting two-sided interferograms actually costs useful measurement time only in those rare cases where the sample is not stable for the minimum time period (or minimum number of flashes) needed to complete a single (double-sided) mirror scan.

A benefit of using the Doubled-Angle phase correction method may be a reduction in the complexity of the hardware needed to measure interferograms. It is not necessary to switch detector preamplifiers and main amplifiers from dc to ac coupling in order to collect a phase spectrum, thus simplifying the instrument configuration. In addition, the requirements of a large dynamic range and a high degree of linearity in the amplification and digitization processes are relaxed. These advantages may also

be realized for a host of other techniques that produce spectra with positive and negative bands, such as vibrational circular dichroism, as well as phase-modulation and lock-in step-scan measurements.

The convolution involved in the Doubled-Angle phase correction method is computationally intensive. For time-resolved step-scan spectroscopy, an interferogram is collected for each time point. Thus, there may be several hundred interferograms from a single experiment. Convolving each of these interferograms with itself during the phase correction process would require a significant amount of time. Additionally, the resulting phase spectra are likely to exhibit errors due to poor signal-to-noise ratio. Instead, it is far better to calculate a single phase spectrum from the average of all the time-resolved interferograms or, better yet, from the first principal component derived by principal component analysis. This phase spectrum can be stored, and then used to correct the phases of the individual interferograms.

The weight of these factors vs. the reduced instrumental requirements of the Doubled-Angle algorithm will determine the relative advantages of direct phase correction vs. use of a dc-coupled stored phase. For instances in which a dc-interferogram can easily be collected, the Doubled-Angle and dc Stored Phase methods can be used in combination, each to double-check the other, since the two methods are susceptible to different sources of error.

ACKNOWLEDGMENTS

The authors would like to thank Galactic Industries, Salem, NH, for permission to publish the relevant parts of the modified icompute.ab Array Basic code. This work was supported by NIH grant GM46854. M.S.H. was supported by NIH Molecular Biophysics Training Grant GM08323.

1. P. Griffiths and J. de Haseth, *Fourier Transform Infrared Spectrometry* (John Wiley and Sons, New York, 1986).
2. L. Mertz, *Transformations in Optics* (John Wiley and Sons, New York, 1965).
3. M. Forman, W. Steel, and G. Vanasse, J. Opt. Soc. Am. **56,** 59 (1966).
4. P. Malon, R. Kobrinskaya, and T. Keiderling, Biopolymers **27,** 733 (1988).
5. E. Lipp and L. Nafie, Biopolymers **24,** 799 (1985).
6. A. Dioumaev and M. Braiman, J. Phys. Chem. B **101,** 1655 (1997).
7. X. Hu, H. Frei, and T. Spiro, Biochemistry **35,** 13001 (1996).
8. C. McCoy and J. de Haseth, Appl. Spectrosc. **42,** 336 (1988).
9. *Bruker Opus Version 3.0* (Bruker Analytische Messtechnik GmbH, Billerica, Massachusetts, 1997).
10. M. Braiman and R. Mathies, Biochemistry **19,** 5421 (1980).
11. M. Braiman, P. Ahl, and K. Rothschild, Proc. Nat. Acad. Sci. U.S.A. **84,** 5221 (1987).

APPENDIX

Modifications of the Array Basic routines supplied with GRAMS/32 software (v. 4.02; Galactic Industries, Salem, NH) were made to implement the new method of phase correction. The changes made to the icompute.ab program to implement the Mertz Signed or Doubled-Angle phase correction method are indicated below. Italics indicate added lines of code. A few lines of the surrounding program are included to mark the locations of the additions. The unitalicized lines are unaltered from the original, except for the conversion of three lines into remarks by addition of the notation REM. Arrows ⇳ mark jumps to different sections of the program.

Mertz Signed Method

```
3020 rfft ph2 : ph2(1)=0 'fft phase array
cmplx2=ph2 : transpose cmplx2 'get 2 rows: real & imag
mag2=sqrt((cmplx2(0)*cmplx2(0))+(cmplx2(1)*cmplx2(1))) 'get magnitude of values
mag2=divrev(mag2,1) 'get 1/magnitude
cmplx2(0)=cmplx2(0)*mag2 : cmplx2(1)=cmplx2(1)*mag2 'normalize
'*************************************************
cmplx2(1)=cmplx2(1)*( cmplx2(0)/abs(cmplx2(0)) ) 'if the real part is <0, then
cmplx2(0)=cmplx2(0)*( cmplx2(0)/abs(cmplx2(0)) ) 'multiply both parts by −1
'*************************************************
cmplx2(1)=−cmplx2(1) 'get complex conjugate
⇳
3070 rfft ph : ph(1)=0 'fft phase array
cmplx=ph : transpose cmplx 'get 2 rows: real & imag
mag=sqrt((cmplx(0)*cmplx(0))+(cmplx(1)*cmplx(1))) 'get magnitude of values
mag=divrev(mag,1) 'get 1/magnitude
cmplx(0)=cmplx(0)*mag : cmplx(1)=cmplx(1)*mag 'normalize
'*************************************************
cmplx(1)=cmplx(1)*( cmplx(0)/abs(cmplx(0)) ) 'if the real part is <0, then
cmplx(0)=cmplx(0)*( cmplx(0)/abs(cmplx(0)) ) 'multiply both parts by −1
'*************************************************
cmplx(1)=−cmplx(1) 'get complex conjugate
```

Doubled-Angle Method

```
'************************************************************ ****
'AC Difference Interferogram compute with zero fill, phasing and apodization.
'Doubled-Angle Phase Correction Algorithm
'************************************************************
'Copyright (c) 1992–98 Galactic Industries Corp. Copy only for use with GRAMS/32®.
```

```
free
pauseoff : onpaint 0
mode = 0 'Stand alone
''portout -44,-1 : debug = 0
'*************************************************************
m=0.1 'get parameters for filter
dialogon ''High-Pass Filter of Interferogram''
dialogask m, 0+256,0,1, ''Breakpoint:''
dialogoff
'*************************************************************
100 dim resfile(256),text(256),temp(256),temp1(256),temp2(256),temp3(256)
⇳
'Find ZPD and set up array for apodization functions
1000 free apdfn : dim apdfn(npts(#s)) 'create apodization func array
if getffp()>getflp() then xflip
if ctype=1 then #s = #s - sum(#s)/pts 'Average subtraction
REM zpd=index0(abs(#s)-max(abs(#s))) 'locate ZPD point
np=npts(#s)
'*************************************************************
free preigram,igram,unapod1 : dim preigram(np),igram(np), unapod1(np)
if getffp()>getflp() then xflip 'make sure that zero is on the left
'**Filter interferogram to remove low-frequency drift
preigram=#s 'transfer to array
filter preigram, 0,0, m,0, m+0.1,1, 1,1 'remove low frequency noise
igram=preigram 'use array limits to zap that added
'by the filtering
'**Self-convolution of interferogram
free temp1 : dim temp1(2*np) 'Array for self-convolution
temp1=0
temp1(np/2,np/2+np-1)=igram(0,np-1) 'zerofill igram on each side
convolve temp1,igram 'Self-convolution
'**Remove apodization effect of self-convoluting boxcars
free unapod1,unapod2 : dim unapod1(np),unapod2(2*np)
unapod1=1
unapod2=0
unapod2(np/2,np/2+np-1)=unapod1(0,np-1)
convolve unapod2,unapod1
unapod1=unapod2/(max(unapod2))
igram=temp1/unapod1
'**Find the ZPD of the convolution
zpd_c=index0(igram-max(igram)) 'Find ZPD of self-convolution
zpd=int ( (zpd_c - (np/2-1))/2 + (np/2-1) ) 'and use to assign zpd of igram
zpd_c=(zpd-(np/2-1))*2 + (np/2-1) 'reassign zpd_c based on zpd
'*************************************************************
if (zpd>=(np/2)-50) then dblside=true else dblside=false
fillbeg -(1/(np-zpd-1))*zpd 'set up fills
fillinc 1/(np-zpd-1)
goto 1100+(apod*100)
⇳
'Linear interpolation of phase
3010 if phint>0 goto 3050
dim ph2(p),ap2(p),cmplx2(p/2,2),mag2(p/2)
REM ph2(0,h)=#s(#zpd,#zpd+h):ph2(p-h,p-1)=#s(#zpd-h,#zpd-1) 'rotate Igram into small phase array
'*************************************************************
ph2(0,h)=igram(zpd_c,zpd_c+h):ph2(p-h,p-1)=igram(zp d_c-h,zpd_c-1) 'rotate Igram into small phase array
'*************************************************************
⇳
3050 REM ph(0,h)=#s(#zpd,#zpd+h):ph(n-h,n-1)=#s(#zpd-h,#zpd-1) 'rotate Igram into big phase array
'*************************************************************
ph(0,h)=igram(zpd_c,zpd_c+h): ph(n-h,n-1)=igram(zpd_c-h,zpd_c-1) 'rotate Igram into big phase array
'*************************************************************
⇳
```

```
'Store phase array if ''Store_new''
'*************************************************************
3100 free cosT, sinT, quad : dim cosT(n/2), sinT(n/2), quad(n/2)
'**Compute half-angles
transpose cmplx
cmplx(1)=cmplx(1)*(-1) 'undo complex conjugate
quad=cmplx(1)<0 '=0 if cmplx(1)>0 and =-1 if cmplx(1)<0
cosT=sqrt (((cmplx(0))*(1) + 1)/2) 'half-angle formulas for cos
sinT=sqrt (((cmplx(0))*(-1) + 1)/2) 'and sin
sinT=sinT*(quad*2 + 1) 'multiply by 1 or -1 to choose proper quadrant
'**Test for flips in the phase array and correct
for j=0 to n/2-2
test1=cosT(j)*cosT(j+1)
test2=sinT(j)*sinT(j+1)
test=test1+test2 'test is cos(T[j]-T[j+1])
if test<0 then flip=-1 else flip=1 'if <0 then T has jumped by >pi/2
cosT(j+1) = flip*cosT(j+1)
sinT(j+1) = flip*sinT(j+1) 'correct for flip
next j
cmplx(0)=cosT 'reassign into phase array
cmplx(1)=sinT
cmplx(1)=cmplx(1)*(-1) 'redo complex conjugate
transpose cmplx
'*************************************************************
if phstr<>2 goto 3200
newspc zqzq(n)
#s=cmplx
```